Water and solute mass balance and circulation model for the rice growing area on the right bank of the lower Guadalquivir River valley

Authors: *Blanca Cuadrado-Alarcón[1], Sébastien Guery[2], Luciano Mateos[1]*

Affiliation: [1] Instituto de Agricultura Sostenible, CSIC, 14004 Córdoba, Spain; [2] Optiriego Consulting, 41015 Sevilla, Spain.

Abstract

The rice-growing area in the right riverbank of the Lower Guadalquivir Marshes (Spain) comprises about 22,000 ha. Land productivity in the region is high due to a favourable environment and high cropping intensity. The rice fields require about 10,000 m^3/ha/year of flood irrigation at a district scale, although individual fields may receive four times as much due to a high rate of surface drainage and water recirculation. Irrigation water is pumped from the Guadalquivir estuary. Salinity is therefore a potential problem which severity depends on the rate of water released from the river reservoirs located upstream and the ocean tides.

A 'bucket' mass balance with capacity constraints has been applied to model daily water, salts balances and circulation in the rice area. The model computes both balances in single irrigation units considering the components evapotranspiration, precipitation, percolation, surface drainage, and irrigation. The connections between the irrigation units requires a conceptualization of the system in a mesh (looped) layout of the distribution network with connection nodes consisting of drains that collect return flows from the irrigation units and supply reused water for irrigation.

Water mass and salt concentration are monitored in specific points of the rice growing area. These measurements were compared with the model outputs. The model was validated by comparing measurements and simulation results from year 2020.

Keywords: 'bucket' model, water balance, salt balance, irrigation, rice.

1. Introduction

Water resources governance needs simple tailormade models adapted to the requirements of each area. This study addresses water management and planning in the rice growing area in the right riverbank of the lower Guadalquivir Marshes, Spain (Figure 1). The area comprises about 22,500 ha between the estuary of the Guadalquivir River and the Doñana National Park. Land productivity in the region is high due to a favourable environment, high cropping intensity and professionalized practices. Rice production is traditional in the region and generates a significant amount of rural employment. The economic activity associated to rice production includes rice industry, agrochemical suppliers, transport, agricultural machinery dealers, and red swamp crayfish (*Procambarus clarkii*) industry.

The fields require about 10,000 m^3/ha/year of irrigation water at a district scale, although individual fields may receive four times as much. This difference is due to a high rate of surface drainage and water recirculation. Irrigation water is pumped from the Guadalquivir estuary.

Water scarcity is the most important limitation to rice production in the Guadalquivir Marshes. The water storage in the basin allowed cultivation of only 50% of the area in 2021 and about 30% in 2022. Moreover, salinity is an additional problem which severity depends on the influence of the ocean tides (greater the further downstream), the water released from the river reservoirs located upstream, and how water is circulated across the district. The water that is not consumed or percolated down to the underlying water table returns to the estuary with an increased concentration of salts. Therefore, salt concentration is spatially distributed across the rice growing area, increasing downstream along the estuary and as the number of upstream water reuses increases.

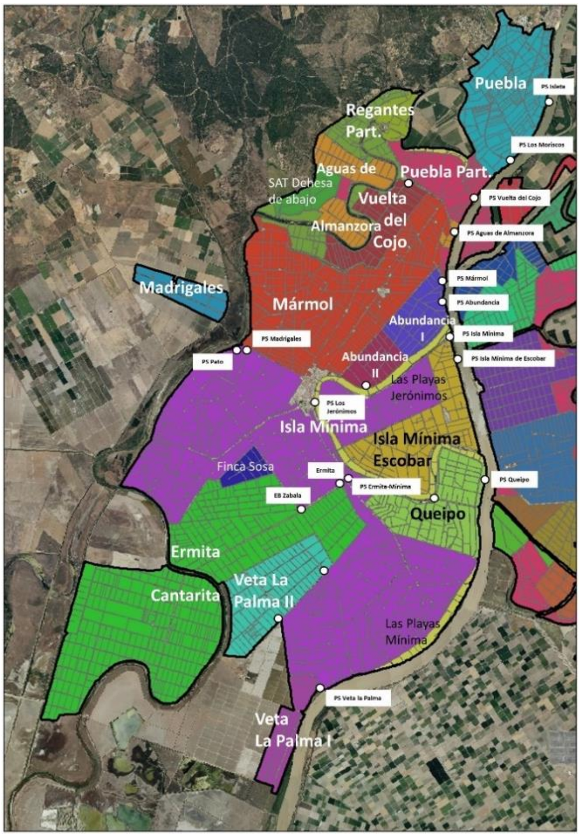

Figure 1. Right riverbank of the rice growing area in the lower Guadalquivir River valley (Spain)

The objective of this paper is the development of a model to predict water and salt distribution in the rice growing area on the right bank of the lower Guadalquivir River, in response to water management and planning decisions.

2. Materials and methods

We developed a model of balance and circulation of water and salt with capacity restrictions to compute daily water and salts distribution in the study area. The model approach (Mateos et al., 2000, Mateos, 2008) computes the water balance in each irrigation and drainage unit in the system considering the components evapotranspiration, precipitation, percolation, surface drainage and irrigation.

The connection between both types of units requires topological conceptualization of the system. In the study case, the arrangement of the units was determined by its mesh layout. Once the water fluxes are computed, salts mass balance equations are formulated for each unit according to its flow diagram, and the unknown salt concentration in every unit is calculated daily.

Volumes of irrigation and drainage are calculated in the irrigation units according to irrigation needs and the management of the drainage outlets. Irrigation and drainage volumes flow from and to different drainage units or the river according to the topological diagram of the system, which is formulated mathematically through two correspondence matrices (Figure 2). The Irrigation Correspondence Matrix (ICM) contains factors that indicate the proportion of irrigation that flows from the water sources (columns) to the irrigation units (rows). The Drainage Correspondence Matrix (DCM) contains factors that indicate the proportion of drainage that flows from each irrigation unit (rows) to the main water source and each drainage units (columns). In the matrices, n is the number of irrigation units represented with the j subscript throughout the model, m is the number of drainage units represented with the k subscript throughout the model, and r is the main water source (Guadalquivir River for this case study).

Irrigation Correspondence Matrix (ICM)

$$
\begin{array}{c|cccccc}
j \backslash k & r & 1 & 2 & 3 & \cdots & m \\
\hline
1 & f_{1r} & f_{11} & f_{12} & f_{13} & \cdots & f_{1k} \\
2 & f_{2r} & f_{21} & f_{22} & f_{23} & \cdots & f_{2k} \\
3 & f_{3r} & f_{31} & f_{32} & f_{33} & \cdots & f_{3k} \\
\vdots & \vdots & \vdots & \vdots & \vdots & \vdots & \vdots \\
n & f_{jr} & f_{j1} & f_{j2} & f_{j3} & \cdots & f_{jk}
\end{array}
$$

Drainage Correspondence Matrix (DCM)

$$
\begin{array}{c|cccccc}
j \backslash k & r & 1 & 2 & 3 & \cdots & m \\
\hline
1 & g_{1r} & g_{11} & g_{12} & g_{13} & \cdots & g_{1k} \\
2 & g_{2r} & g_{21} & g_{22} & g_{23} & \cdots & g_{2k} \\
3 & g_{3r} & g_{31} & g_{32} & g_{33} & \cdots & g_{3k} \\
\vdots & \vdots & \vdots & \vdots & \vdots & \vdots & \vdots \\
n & g_{jr} & g_{j1} & g_{j2} & g_{j3} & \cdots & g_{jk}
\end{array}
$$

Figure 2. Correspondence matrices derived from the conceptualization of the system

Factors f and g must meet conditions:

$$\forall\, j\,; \qquad f_{jr} + \sum_{k=1}^{m} f_{jk} = 1 \qquad (1a)$$

$$\forall\, j\,; \qquad g_{jr} + \sum_{k=1}^{m} g_{jk} = 1 \qquad (1b)$$

2.1. Water balance in the irrigation units

The water mass balance equation for an irrigation unit is:

$$\boldsymbol{V_{ij}} = \boldsymbol{V_{(i-1)j}} - \boldsymbol{ETc_{ij}} + \boldsymbol{R_{ij}} + \boldsymbol{I_{ij}} - \boldsymbol{D_{ij}} - \boldsymbol{P_{ij}} \qquad (2)$$

Where the i subscript represents the day in the balance, the *j* subscript represents the irrigation unit, $\boldsymbol{V_{ij}}$ and $\boldsymbol{V_{(i-1)j}}$ are the volumes of water in the unit *j* on the day of concern and the previous day, respectively, and $\boldsymbol{ETc_{ij}}$, $\boldsymbol{R_{ij}}$, $\boldsymbol{I_{ij}}$, $\boldsymbol{D_{ij}}$,and $\boldsymbol{P_{ij}}$ are the volumes of crop evapotranspiration, rainfall, irrigation, surface drainage, and percolation, respectively, in the irrigation unit *j* on day *i.*

$\boldsymbol{ETc_{ij}}$ was calculated with the FAO Penman-Monteith method (Allen et al., 1998). Daily reference evapotranspiration (ETo_i) was taken from the Isla Mayor weather station part of the Agroclimatic Information Network of Andalusia (RIA, acronym of the name in Spanish, www.juntadeandalucia.es/agriculturaypesca/ifapa/ria/), which is located in the study area. The daily crop coefficient (kc_{ij}) was considered to be 1.05 when the irrigation unit is flooded and before rice plants emerge above the water surface, 1.20 when the crop is fully developed, and 0.6 just before harvest (Allen et al., 1998). Satellite Sentinel-2 images of the study area, downloaded from the Copernicus open-access website (https://sci-hub.copernicus.eu), were used to derive unit specific crop coefficients derived from the vegetation index NDVI (Mateos et al., 2013; González-Dugo et al., 2013). During the water filling period, that in large irrigation units may take several days, a filling factor (varying from 0 to 1) simulating the flooding progression is multiplied by the corresponding ETc_{ij}. The daily filling progression factor ($FillF_{ij}$) is calculated based on the pumping capacity in the irrigation unit and the irrigation needs of the day.

$$ETc_{ij} = ETo_i * kc_{ij} * Area_j * FillF_{ij} \qquad (3)$$

$\boldsymbol{R_{ij}}$ was calculated from rainfall data recorded at the Isla Mayor weather station.

$\boldsymbol{V_{ij}}$, $\boldsymbol{I_{ij}}$, $\boldsymbol{D_{ij}}$,and $\boldsymbol{P_{ij}}$ are functions of the water depth in the irrigation unit ($\boldsymbol{h_{ij}}$), which is the water depth in the soil profile ($\boldsymbol{h_{SWCij}}$) plus the water depth in the free water layer above the soil surface ($\boldsymbol{h_{FWDij}}$):

$$\boldsymbol{h_{ij}} = \boldsymbol{h_{SWCij}} + \boldsymbol{h_{FWDij}} \qquad (4)$$

The value of $\boldsymbol{h_{SWCij}}$ can vary between the soil water depth in the soil profile at wilting point (h_{WPj}) and at saturation water content (h_{SATj}), passing by that at field capacity (h_{FCj}). Wilting point, saturation water content and field capacity are soil parameters specific of each irrigation unit. The soil profile was considered 1 m deep for this specific application of the model purpose. Thus:

$$V_{ij} = Area_j * h_{ij} \qquad (5)$$

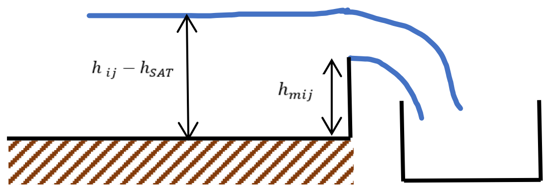

Figure 3. Sketch of an outlet in the Guadalquivir case study irrigation unit

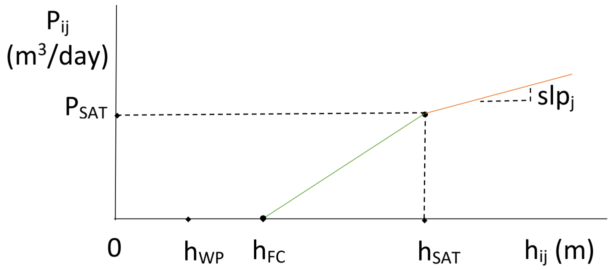

Figure 4. Relationship between percolation and water height

$\boldsymbol{D_{ij}}$ for the Guadalquivir case study is calculated using the discharge equation of a rectangular weir with h_{ij} as independent variable (Fig. 4):

$$D_{ij} = 86400 * \frac{3}{2} * \sqrt{2g} * C_d * B_{tj} * \left(h_{ij} - h_{SATj} - h_{mij}\right)^{3/2} \qquad \text{If } h_{ij} > \left(h_{mij} + h_{SATj}\right) \qquad (6a)$$

$$D_{ij} = 0 \qquad \text{If } h_{ij} \leq \left(h_{mij} + h_{SATj}\right) \qquad (6b)$$

Where $D_{ij}$is expressed in m^3 day^{-1}, B_{tj} is the width of weir crest (m) in unit *j*, estimated as 0.20 m ha^{-1}, C_d is the discharge coefficient of the weir, and h_{mij} is a management parameter equal to de height of the weir crest on day *i*, unit *j*.

$\boldsymbol{P_{ij}}$ is calculated using a three-branch linear equation with h_{ij} as independent variable (Figure 4):

$$P_{ij} = 0 \qquad \text{If } h_{ij} < h_{FCj} \qquad (7a)$$

$$P_{ij} = FillF_{ij} * P_{SATj} * \left(h_{ij} - h_{FCj}\right)/\left(h_{SATj} - h_{FCj}\right) \qquad \text{If } h_{SATj} > h_{ij} \geq h_{FCj} \qquad (7b)$$

$$P_{ij} = FillF_{ij} * \left(P_{SATj} + slp_j * \left(h_{ij} - h_{SATj}\right)\right) \qquad \text{If } h_{ij} \geq h_{SATj} \qquad (7c)$$

Where slp_j is the slope for the increase in percolation rate due to a free water layer above the saturated soil (Fig. 5). Note that the filling factor used to adjust ETc_{ij} during the flooding progression is also applied to P_{ij}.

$\boldsymbol{I_{ij}}$ is calculated as the amount of water needed to reach the target free water depth ($TFWD_{ij}$), which is a management daily input value representing the depth of water above the soil surface that is desired in the irrigation unit. $\boldsymbol{I_{ij}}$ is constrained by the pumping capacity (B_{maxj}) in the irrigation unit. Thus, $\boldsymbol{I_{ij}}$ can be expressed as a function of the independent variable h_{ij} as:

$$I_{ij} = 0 \qquad \text{If } h_{ij} \geq \left(TFWD_{ij} + h_{SATj}\right) \text{ or } TFWD_{ij} = 0 \qquad (8a)$$

$$I_{ij} = \left(TFWD_{ij} + h_{SATj} - h_{ij}\right) * Area_j \qquad \text{If } h_{ij} < \left(TFWD_{ij} + h_{SATj}\right) \qquad (8b)$$

$$I_{ij} = B_{maxj} \qquad \text{If } I_{ij} > B_{maxj} \qquad (8c)$$

I_{ij} and D_{ij} are divided according to their sources and destinations using the factors in ICM and DCM, respectively:

$$I_{ij} = \sum_{k=1}^{m}(I_{ij} * f_{jk}) + I_{ij} * f_{jr} \qquad (9a)$$

$$D_{ij} = \sum_{k=1}^{m}(D_{ij} * g_{jk}) + D_{ij} * g_{jr} \qquad (9b)$$

Substituting equations 5, 6, 7 and 8 into equation 2, the later becomes a non-linear function that can be solved for h_{ij} applying the Newton-Raphson method.

2.2. Water balance in the drainage units

The drainage ditches act as water reservoirs, accumulating drainage water from the irrigation units to be evacuated or reused for irrigation. The dimensions of the drainage units are input to the model. The water balance of the drainage units may be expressed as:

$$V_{ik} = V_{(i-1)k} - E_{ik} - P_{ik} + R_{ik} + \sum_{j=1}^{n} D_{ij} * g_{jk} - \sum_{j=1}^{n} I_{ij} * f_{jk} + F_{in\ ik} - F_{out\ ik} \qquad (10)$$

Where the subscript i indicates the daily step and the subscript k indicates the drainage unit. $\boldsymbol{V_{ik}}$ and $\boldsymbol{V_{(i-1)k}}$ are the volumes of water in the unit k on days i and i-1, respectively. $\boldsymbol{E_{ik}}$, $\boldsymbol{R_{ik}}$, and $\boldsymbol{P_{ik}}$ are the volumes of evaporation from the drain water surface, rainfall on the drain and percolation through the drain wetted perimeter, respectively, for drainage unit k on day i. $\boldsymbol{F_{in\ ik}}$ and $\boldsymbol{F_{out\ ik}}$ are the daily water flows in drainage unit k entering from and discharging to the main source (the river in the case study), respectively.

V_{ik}, E_{ik}, P_{ik}, $F_{in\ ik}$ and $F_{out\ ik}$ are functions of the water depth in the drainage unit (h_{ik}), which is the water depth stored in the drainage ditch. The drains are assumed of trapezoidal cross-section (Figure 5). Values for the base of the cross-section (b_k), slope of the sides (z_k), maximum water depth (y_k), maximum width (T_k), and length of the unit (L_k) are input parameters. R_{ik} is calculated with surface T_k, and the precipitation of the weather station mentioned in section 2.1.

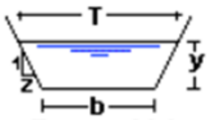

Figure 5. Trapezoidal cross section of a drainage unit

$\boldsymbol{V_{ik}}$ is expressed as:

$$V_{ik} = (b_k + z_k * h_{ik}) * h_{ik} * L_k \qquad (11)$$

$\boldsymbol{E_{ik}}$ is calculated from ET_0, an open water evaporation coefficient (k), L_k, and the free water surface, which is a function of h_{ik}:

$$E_{ik} = ET_{0_i} * k * L_k * (b_k + 2 * z_k * h_{ik}) \qquad (12)$$

$\boldsymbol{P_{ik}}$ is estimated from a rate of percolation for the saturated drains ($K_{sat\ k}$), L_k and the wetted perimeter, which is a function of h_{ik}.

$$P_{ik} = K_{sat\ k} * \mathrm{L}_k * \left(b_k + 2 * h_{ik} * \sqrt{1 + z_k^2}\right) \qquad (13)$$

$\boldsymbol{F_{out\ ik}}$ is the volume of water that exceeds the drainage unit capacity ($V_{max\ k}$), and thus it is returned to the source:

$$F_{out\ ik} = V_{ik} - V_{max\ k} \qquad \text{If } V_{ik} > V_{max\ k} \qquad (14a)$$

$$F_{out\ ik} = 0 \qquad \text{If } V_{ik} \leq V_{max\ k} \qquad (14b)$$

During periods of high tides, the drainage units can take up water from the source. This flow ($\boldsymbol{F_{in\ ik}}$) is computed as the volume needed to fill the drainage in one day up to a fraction (q) of $V_{max\ k}$:

$$F_{in\ ik} = 0 \qquad \text{If } V_{ik} \geq q * V_{max\ k} \qquad (15a)$$

$$F_{in\ ik} = q * V_{max\ k} - V_{ik} \qquad \text{If } V_{ik} < q * V_{max\ k} \qquad (15b)$$

The fraction q is assumed to be 0.1 in all the drainage units. Equation 15 is a very rough approximation justified by the current limited knowledge of the drains hydraulics.

Substituting equations 11, 12, 13, 14 and 15 into equation 10, the later becomes a non-linear function on h_{ik} that can be solved applying the Newton-Raphson method.

2.3. Solute balance equations and salt concentration calculation

The solute mass conservation equation for the irrigation and drainage units are:

$$V_{ij} * c_{ij} = V_{(i-1)j} * c_{(i-1)j} - P_{ij} * c_{ij} - D_{ij} * c_{ij} + \sum_{k=1}^{m}(I_{ij} * f_{jk} * c_{ik}) + I_{ij} * f_{jr} * c_{ijr} \quad (16)$$

$$V_{ik} * c_{ik} = V_{(i-1)k} * c_{(i-1)k} - P_{ik} * c_{ik} + F_{in\,ik} * c_{ikr} - F_{out\,ik} * c_{ik} - c_{ik} * \sum_{j=1}^{n}(I_{ij} * f_{jk}) + \sum_{j=1}^{n}(D_{ij} * g_{jk} * c_{ij}) \quad (17)$$

Where $\boldsymbol{c_{ij}}$ is the solute concentration in the irrigation unit j on day i, and $\boldsymbol{c_{ik}}$ is the solute concentration in the drainage unit k on day i. $\boldsymbol{c_{ijr}}$ or $\boldsymbol{c_{ikr}}$ are the concentration of solutes on day i for the stretch of the external source (the river water) where the irrigation unit j or drainage unit k are connected.

There are as many solute balance equations as there are irrigation plus drainage units, while the unknowns are the concentration of solutes in each unit. The system of linear equations is solved applying the Gaussian elimination method using the LAPACK routine (Anderson et al., 1999) in the NumPy library linear algebra submodule (Harris et al., 2020).

3. Results and discussion

The topological diagram of the hydraulic arrangement for the 'bucket' modelling approach applied to the rice growing area in the right riverbank of the Lower Guadalquivir valley is in Figure 6.

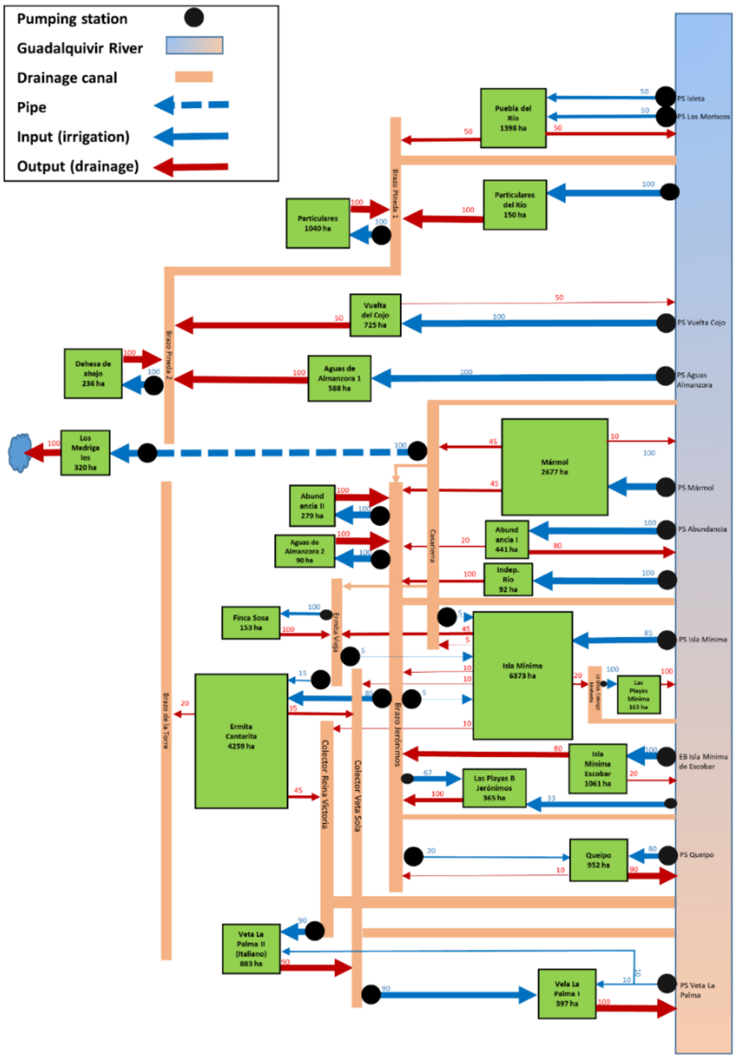

Figure 6. Conceptual layout for the bucket mass balance model in the Guadalquivir case study

Figure 7 shows the daily evolution of the water balance components and input and output salt concentrations in one example irrigation unit. The sharp initial increase of irrigation corresponds to the filling of the irrigation unit, while the other sudden changes are due to variations of the management free water depth and the management height of the drainage weir crest ($TFWD_{ij}$ and h_{mij}, respectively). Water balances for every irrigation unit during irrigation season 2020 (Table 1) resulted on average irrigation of 2500 mm, and average surface drainage fraction (SDF) of 0.52. SDF is calculated as the fraction of irrigation that leaves the unit by surface drainage, and thus is susceptible for water recirculation.

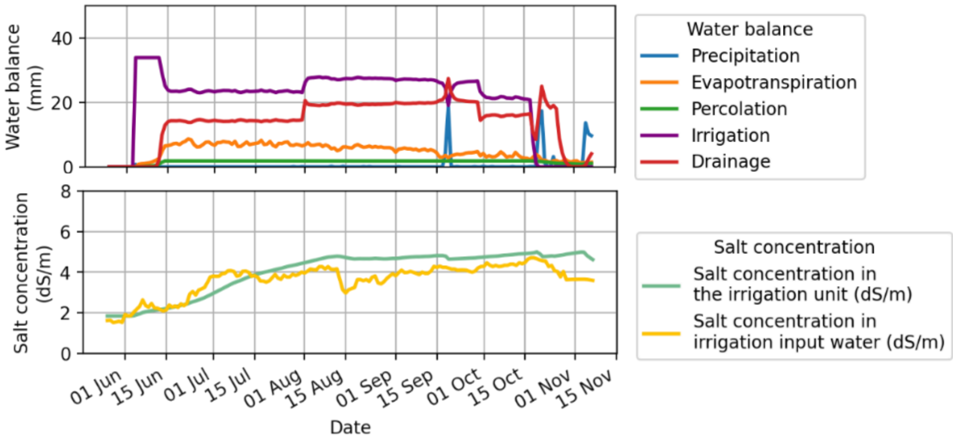

Figure 7. Results of the daily evolution of water and salinity in the irrigation unit called Isla Minima for the irrigation season 2020

Table 1. Modelled total values for the water balance during year 2020

Irrigation unit	ETc (mm)	Rainfall (mm)	Percolation (mm)	Surface drainage (mm)	Irrigation (mm)	SDF
IslaMinima	796	97	266	2,365	3,474	0.68
AbundanciaI	853	97	279	1,917	3,091	0.62
AbundanciaII	770	97	267	922	2,008	0.46
IslaMinimaEscobar	779	97	266	2,146	3,240	0.66
Poblado	824	97	272	2,630	3,771	0.70
Marmol	809	97	268	2,617	3,740	0.70
ErmitaCantarita	796	97	267	2,609	3,720	0.70
PueblaRio	818	97	276	894	2,032	0.44
Madrigales	757	97	259	1,654	2,718	0.61
VueltaCojo	770	97	265	476	1,557	0.30
VetaPalmaII	784	97	273	1,380	2,489	0.55
PartRio	790	97	270	891	1,997	0.45
Particulares	777	97	268	900	1,992	0.45
AguasAlmanzoraA	806	97	271	848	1,967	0.43
VetaPalmaI	887	97	291	1,169	2,389	0.49
DehesaAbajo	770	97	268	884	1,970	0.45
PlayasJeronimos	757	97	266	891	1,963	0.45
PlayasMinima	763	97	267	895	1,974	0.45
AguasAlmanzoraB	770	97	267	913	1,999	0.46
FincaSosa	757	97	266	890	1,962	0.45

The percentages of water inputs and outputs in the study area are in Figure 8. 77.6% of the inputs was water pumped from the river, and 45.1% of the outputs was flowed back to the Guadalquivir River.

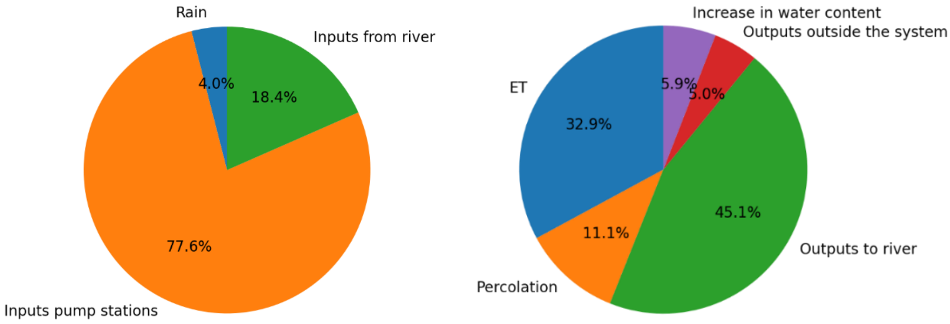

Figure 8. Modelled fractions inputs and outputs in the rice growing right riverbank of the Guadalquivir lower valley for year 2020

To validate the water balance model, measured data of water inputs from the 9 pumping stations located in the Guadalquivir River (https://www.chguadalquivir.es/saih/) were compared with the corresponding model outputs (Table 2). A difference of a 6 % in total volumes measured and modelled is observed.

Table 2. Comparison of measured and simulated values

River pumping stations	Measured values (m3)	Simulated values (m3)	River pumping stations	Measured values (m3)	Simulated values (m3)
PueblaRio	28,750,288	21,528,785	**IslaMinima**	185,008,048	172,896,432
VueltaCojo	9,944,227	9,702,694	**IslaMinimaEscobar**	32,358,298	32,608,715
AguasAlmanzoraA	11,298,381	9,453,351	**Ermita**	148,443,905	147,381,739
Marmol	96,584,383	89,784,852	**Poblado**	28,381,226	25,845,170
Abundancial	15,902,765	12,558,145			

Salt concentration in the irrigation units increases during the irrigation season, and starts decreasing with precipitations in November (Figure 7). This is because salinity of the water that enters the system increases during the summer season, and the evaporation process concentrates salt content. Table 3 contains simulated mean concentration of salt in the irrigation water and in the irrigation unit.

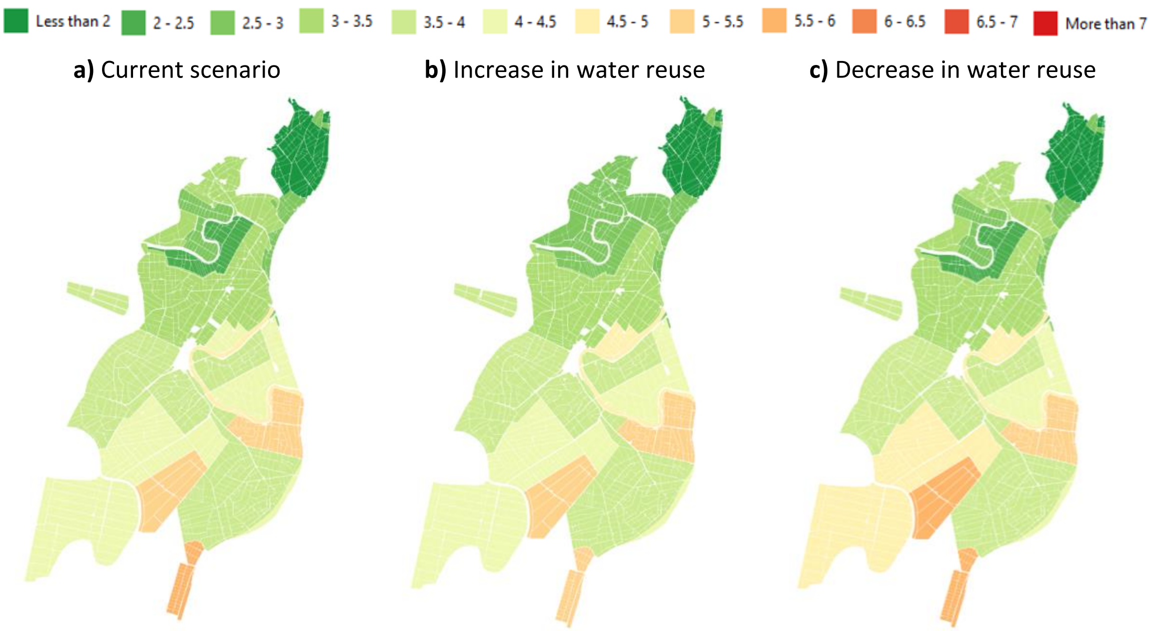

Figure 9. Spatial distribution of salinity in the input water for irrigation. Average value for year 2020 (dS/m). Rice growing right riverbank of the lower Guadalquivir valley.

Table 3. Modelled salt concentration values for the water balance during year 2020

Irrigation unit	Irrigation input (dS/m)	Irrigation unit (dS/m)	Irrigation unit	Irrigation input (dS/m)	Irrigation unit (dS/m)
IslaMinima	3.7	4.0	**VetaPalmalI**	5.4	6.5
AbundanciaI	3.3	3.8	**PartRio**	2.5	3.0
AbundanciaII	4.4	4.9	**Particulares**	3.1	3.4
IslaMinimaEscobar	4.5	4.8	**AguasAlmanzoraA**	2.8	3.4
Poblado	5.0	5.4	**VetaPalmal**	5.6	7.0
Marmol	3.2	3.5	**DehesaAbajo**	3.1	4.6
ErmitaCantarita	4.4	4.7	**PlayasJeronimos**	4.6	4.6
PueblaRio	1.9	2.4	**PlayasMinima**	4.3	4.6
Madrigales	3.74	3.99	**AguasAlmanzoraB**	4.44	4.57
VueltaCojo	2.50	3.11	**FincaSosa**	4.13	4.58

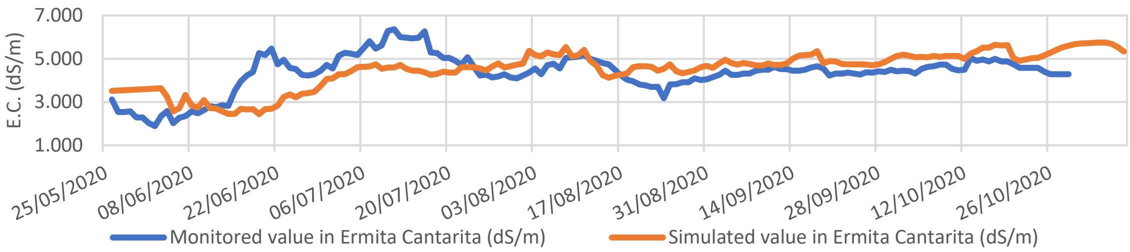

Figure 10. Monitored and simulated salinity in Ermita Cantarita, year 2020

Figure 9a shows the distribution of averaged salinity for the growing season under the management practices in 2020. Overall, it may me observed an increase of salinity from north to south, determined by the salinity of the river water and irrigation reusing drainage water.

Simulated daily measurements of salinity at the pumping station Ermita Cantarita, that reuses drainage water (Figure 1), were compared with daily measurements (Figure 10). Mean seasonal simulated and measured salinity were equal (4.4 dS/m).

Alternative management practices may be simulated to evaluate potential improvements. Figure 9 shows also simulated salinity results assuming an increase in water reuse, obtaining an average input irrigation in the irrigation units of 4005 mm and a surface drainage fraction of 0.72 (Figure 9b) and a reduction on water reuse (Figure 9c), obtaining an average input irrigation in the irrigation units of 1940 mm and a surface drainage fraction of 0.4. Comparing the three maps in Figure 9, there is a clear effect of salt redistribution when we increase water reuse within the system. Salinity in areas with higher concentration is attenuated, and areas with relatively low salinity increase their value.

4. Conclusions

A ‘bucket’ water and salt mass balance model has been set up for the rice growing area in the right riverbank of the Guadalquivir lower valley, with an area of 22,500 ha. The main difficulty was found in the interconnections of the system, being a large and complex network with supply, drainage and water reuse.

Results show good agreement with measured values, the average irrigation input in the irrigation units is 2500 mm with a surface drainage fraction of 0.52, which indicates fraction of irrigation that leaves the unit by surface drainage, and is susceptible for recirculation within the system. Average salinity is 4.4 dS/m, with a value of 1.9 dS/m in the irrigation unit located upsteam, and increasing downstream along the Guadalquivir River.

The model allows the simulation of different water management practices to evaluate possible improvements in the performance of the entire area.

Acknowledgements: This work is included in the framework of the MEDWATERICE project *Towards a sustainable water use in Mediterranean rice-based agro-ecosystems*, funded by the PRIMA program (Agencia Estatal de Investigación, PCI2019-103714), the ORYZONTE project, and the WAGRINNOVA project *Co-innovations across scales to enhance sustainable intensification in water-managed agricultural systems in West Africa*, funded by LEAP-Agri (Agencia Estatal de Investigación, PCI2018-093051).

References

Allen, R.G., Pereira, L.S., Raes, D. and Smith, M., (1998). Crop evapotranspiration - Guidelines for computing crop water requirements. *FAO Irrigation and Drainage Paper 56*. FAO, Rome.

Anderson, E., Bai, Z., Bischof, S., C. and Blackford, Demmel, J., Dongarra, J., J. and Du Croz, Greenbaum, A., … Sorensen, D. (1999). LAPACK Users' Guide (Third). Philadelphia, PA: Society for Industrial and Applied Mathematics.

González-Dugo, M.P., Escuin, S., Cano, F., Cifuentes, V., Padilla, F.L.M., Tirado, J.L., Oyonarte, N., Fernández, P. and Mateos L., (2013) Monitoring evapotranspiration of irrigated crops using crop coefficients derived from time series of satellite images. II. Application on basin scale. *Agricultural Water Management*. 125: 92-104

Harris, C. R., Millman, K. J., van der Walt, S. J., Gommers, R., Virtanen, P., Cournapeau, D., … Oliphant, T. E. (2020). Array programming with NumPy. *Nature*, 585, 357–362.

Mateos L, Young CA, Wallender WW, Carlson HL (2000) Simulating spatially distributed water and salt balances. *J Irrig Drain Engrg* 126:288–295

Mateos, L. (2008) Identifying a new paradigm for irrigation system performance. Irrigation Science 27:25-34

Mateos, L., González-Dugo, M.P., Testi, L., Villalobos, F.J., (2013) Monitoring evapotranspiration of irrigated crops using crop coefficients derived from time series of satellite images. I. Method validation. *Agricultural Water Management*. 125: 81-91